JOURNAL OF COMPUTATIONAL PHYSICS 30, 389–406 (1979)

Stability Analysis for MacCormack's Time-Splitting Technique Applied to a Model Conduction Problem

EVERETT JONES

Department of Aerospace Engineering, University of Maryland, College Park, Maryland 20742

Received December 27, 1977; revised May 31, 1978

A stability analysis was developed for the time-split method of MacCormack [7] and [8] as applied to a model conduction problem with motion of the continuum. Extrema in the magnitude of the amplification factors for variations in wave numbers were found and used to define the stability boundaries of the operators. Numerical experiments verified this analysis. A simplified form of the stability boundary was demonstrated and should be a practical guide for the conduction problem considered.

I. INTRODUCTION

In a recent investigation [1], a modification of MacCormack's method [2] for the time dependent solution of the Navier-Stokes equations was applied to investigate laminar and turbulent mixing of bounded parallel streams. This numerical method was also applied to model conduction problems with similar boundary conditions and a uniformly moving medium. Solutions for transient conduction problems and steady laminar mixing of a single species fluid compared very well with exact solutions. Solutions were also obtained for turbulent mixing of a single species fluid but neither exact solutions or data were available for comparison. Therefore, test cases were chosen to compare as close as possible with the results of Borghi and Charpenel [3]. Results appeared good for inlet profiles having smooth variations with continuous derivatives of flow variables across the entire inlet. However, for inlet profiles more nearly approximating the small or zero thickness mixing region between two parallel streams, the time variations of properties appeared to persist indefinitely.

The steady flow solutions of [1], as for most published solutions using MacCormacks method [2], are obtained by computing the flow at large times after it develops from an initial guess for the solution. Therefore, the correct transient behavior js not of primary interest while the approach to the steady state solution is extremely important. However, the flow inside an internal combustion engine is intrinsically transient and computations [4] and [5] of this flow must have the proper transient behavior.

In a continuation of the investigations reported in [1], the programs were modified to study turbulent mixing of two streams of different chemical species without chemical or vibrational kinetics because data became available for this case. As above, results

0021-9991/79/030389–18$02.00/0

for steady flow could not be obtained and the cause appeared to be the numerical instability of the computational algorithms.

Since the model conduction problem involves only one differential equation instead of the system of four or six equations required for the fluid mechanics programs, the stability of the algorithm for the conduction program was investigated first. It should be noted that the conduction equation contained a term producing convection with constant velocity and therefore has the same form as the linearized form of the flow equations actually used in a stability analysis of the fluid mechanic equations.

Several versions or modifications of the earlier MacCormack algorithm [2] for the conduction problem were investiigated using a modification of the von Neumann stability analysis [6]. The amplification factor for the Fourier components of a perturbation was found for each of the several algorithms considered. The extrema in magnitude of the amplification factor for all Fourier components were found. Then, the stability boundary was determined by the condition that the largest magnitude for all maxima does not exceed one. This procedure required that a common region for the time increment exist for four different combinations of odd and even Fourier components for waves in the two coordinate directions. A surprising result was the occurrence of a lower bound on time step. Unfortunately, none of the algorithms studied was stable in this context despite the fact that stable solutions were obtained [1] using these algorithms.

Even though the stability analysis of the conduction algorithms is simplified by the presence of only one differential equation, the analytical results are sufficiently complex that the exact cause of this result was not apparent. It was clear that the complexity would be significantly reduced if some of the requirements could be decoupled.

Since the original MacCormack algorithm [2] was introduced, MacCormack [7] has also applied a time-split method in which the solution is advanced in time individually by separate operators. One operator used only variations in one spatial coordinate while the other operator used only variations in the other spatial coordinate. Stability of each operator then dictated its time step and the desired decoupling was obtained. The investigation reported here applies the previous stability method to a time splitting algorithm for the model conduction problem.

II. The Stability Analysis

A. *The Conduction Problem and the Analytical Solution*

The physical problem of interest has a continua moving at constant velocity u parallel to the x axis. Initially, the temperature T is constant, T_∞, but for later time the inlet temperature profile has a constant jump for all y, $(\delta T)_1$, and a cosine variation in y, $(\delta T)_2 \cos(\pi y)$. Symmetry conditions are applied on the upper ($y = 1$) and lower ($y = 0$) boundaries. In summary, the nondimensional form of the boundary value problem is:

$$\frac{\partial T}{\partial t} + \beta \frac{\partial T}{\partial x} = \frac{\partial^2 T}{\partial x^2} + \frac{\partial^2 T}{\partial y^2} \tag{1}$$

$$T(x, y, 0) = T_\infty \tag{2}$$

$$T(0, y, t) = g(y) = T_\infty + (\delta T)_1 + (\delta T)_2 \cos(\pi y) \tag{3}$$

$$T(x, y, t) = T_\infty \qquad \text{for infinite } x \tag{4}$$

$$\frac{\partial T}{\partial y}(x, 0, t) = 0 = \frac{\partial T}{\partial y}(x, 1, t) \tag{5}$$

x and y are referenced to the physical height of the region, L. Temperature has an arbitrary reference and time has the reference

$$t_R = \left(\frac{\rho c}{k}\right) L^2 \tag{6}$$

where ρ, c and k are constant and are the dimensional values of density, specific heat and conductivity for the continua. β is the nondimensional velocity parameter

$$\beta = \frac{u t_R}{L} \tag{7}$$

The analytical solution of this initial boundary value problem is:

$$\begin{aligned} T(x, y, t) = T_\infty &+ \frac{1}{2}(\delta T)_1 \left[\mathrm{ERFC}\left(\frac{x}{2(t)^{1/2}} - \frac{\beta}{2} t^{1/2}\right)\right. \\ &\left. + e^{\beta x}\, \mathrm{ERFC}\left(\frac{x}{2(t)^{1/2}} + \frac{\beta}{2} t^{1/2}\right)\right] \\ &+ \frac{1}{2}(\delta T)_2\, e^{\beta x/2} \left[e^{-R_1 x}\, \mathrm{ERFC}\left(\frac{x}{2(t)^{1/2}} - R_1 (t)^{1/2}\right)\right. \\ &\left. + e^{R_1 x}\, \mathrm{ERFC}\left(\frac{x}{2(t)^{1/2}} + R_1 (t)^{1/2}\right)\right] \cos \pi y \end{aligned} \tag{8}$$

where

$$R_1^2 = \left(\frac{\beta}{2}\right)^2 + \pi^2 \tag{9}$$

B. *The Time-Split Algorithm*

The conduction equation can be written in the conservation form:

$$\frac{\partial T}{\partial t} + \frac{\partial F}{\partial x} + \frac{\partial G}{\partial y} = 0 \tag{10}$$

where

$$F = \beta T - \frac{\partial T}{\partial x}, \qquad G = -\frac{\partial T}{\partial y} \tag{11}$$

The computational net chosen has constant spatial increments with:

$$x_j = j\,\Delta x, \qquad j = 0, 1, 2, \ldots, \frac{x_{\max}}{\Delta x} \tag{12a}$$

$$y_k = k\,\Delta y, \qquad k = 0, 1, 2, \ldots, \frac{1}{\Delta y} \tag{12b}$$

Then, for the time-split method [7], the temperature at x_j and y_k can be advanced in time by two operators.

$$T^{**}_{j,k} \equiv T_{j,k}(t + (\Delta t)_x) = L_x(\Delta t)_x\, T^{*}_{j,k}, \qquad T^{*}_{j,k} \equiv T_{j,k}(t) \tag{13a}$$

or

$$T^{**}_{j,k} \equiv T_{j,k}(t + (\Delta t)_y) = L_y(\Delta t)_y\, T^{*}_{j,k}, \qquad T^{*}_{j,k} \equiv T_{j,k}(t) \tag{13b}$$

The $L_x(\Delta t)_x$ operator for MacCormack's time-split method [7] can be given by the sequence below using a predictor-corrector method:

$$\left(\frac{\partial T}{\partial t}\right)^{*}_{j,k} \equiv (\overline{T}^{**}_{j,k} - T^{*}_{j,k})/(\Delta t)_x = -(F^{*}_{j,k} - F^{*}_{j-1,k})/(\Delta x) \tag{14a}$$

with

$$F^{*}_{j,k} = \beta T^{*}_{j,k} - (T^{*}_{j+1,k} - T^{*}_{j,k})/(\Delta x) \tag{14b}$$

and

$$\left(\overline{\frac{\partial T}{\partial t}}\right)^{**}_{j,k} = -(\overline{F}^{**}_{j+1,k} - \overline{F}^{**}_{j,k})/(\Delta x) \tag{14c}$$

with

$$\overline{F}^{**}_{j,k} = \beta \overline{T}^{**}_{j,k} - (\overline{T}^{**}_{j,k} - \overline{T}^{**}_{j-1,k})/(\Delta x) \tag{14d}$$

Finally,

$$(T^{**}_{j,k} - T^{*}_{j,k})/(\Delta t)_x = \frac{1}{2}\left[\left(\frac{\partial T}{\partial t}\right)^{*}_{j,k} + \left(\overline{\frac{\partial T}{\partial t}}\right)^{**}_{j,k}\right] \equiv \left[\left(\overline{\frac{\partial T}{\partial t}}\right)^{*}_{j,k}\right]_x \tag{14e}$$

Alternatively, the spatial differences above can be reversed in each step with

$$\left(\frac{\partial T}{\partial t}\right)^{*}_{j,k} \equiv (\overline{T}^{**}_{j,k} - T^{*}_{j,k})/(\Delta t)_x = -(F^{*}_{j+1,k} - F^{*}_{j,k})/(\Delta x) \tag{15a}$$

where

$$F^{*}_{j,k} = \beta T^{*}_{j,k} - (T^{*}_{j,k} - T^{*}_{j-1,k})/(\Delta x) \tag{15b}$$

and

$$\left(\overline{\frac{\partial T}{\partial t}}\right)^{**}_{j,k} = -(\overline{F}^{**}_{j,k} - \overline{F}^{**}_{j-1,k})/(\Delta x) \tag{15c}$$

where

$$\bar{F}^{**}_{j,k} = \beta \bar{T}^{**}_{j,k} - (\bar{T}^{**}_{j+1,k} - \bar{T}^{**}_{j,k})/(\Delta x) \tag{15d}$$

Then

$$(T^{**}_{j,k} - T^{*}_{j,k})/(\Delta t)_x = \frac{1}{2}\left[\left(\frac{\partial T}{\partial t}\right)^{*}_{j,k} + \left(\overline{\frac{\partial T}{\partial t}}\right)^{**}_{j,k}\right] \equiv \left[\left(\overline{\frac{\partial T}{\partial t}}\right)^{**}_{j,k}\right]_x \tag{15e}$$

The $L_y(\Delta t)_y$ operator is given by the following sequence where a predictor-corrector method is again used:

$$\left(\frac{\partial T}{\partial t}\right)^{*}_{j,k} \equiv (\bar{T}^{**}_{j,k} - T^{*}_{j,k})/(\Delta t)_y = -(G^{*}_{j,k} - G^{*}_{j,k-1})/(\Delta y) \tag{16a}$$

with

$$G^{*}_{j,k} = -(T^{*}_{j,k+1} - T^{*}_{j,k})/(\Delta y) \tag{16b}$$

and

$$\left(\overline{\frac{\partial T}{\partial t}}\right)^{**}_{j,k} = -(\bar{G}^{**}_{j,k+1} - \bar{G}^{**}_{j,k})/(\Delta y) \tag{16c}$$

with

$$\bar{G}^{**}_{j,k} = -(\bar{T}^{**}_{j,k} - \bar{T}^{**}_{j,k-1})/(\Delta y) \tag{16d}$$

Finally,

$$(T^{**}_{j,k} - T^{*}_{j,k})/(\Delta t)_y = \frac{1}{2}\left[\left(\frac{\partial T}{\partial t}\right)^{*}_{j,k} + \left(\overline{\frac{\partial T}{\partial t}}\right)^{**}_{j,k}\right] \equiv \left[\left(\overline{\frac{\partial T}{\partial t}}\right)^{*}_{j,k}\right]_y \tag{16e}$$

As with the L_x operator the spatial differences above can all be reversed to produce the following system of equations:

$$\left(\frac{\partial T}{\partial t}\right)^{*}_{j,k} \equiv (\bar{T}^{**}_{j,k} - T^{*}_{j,k})/(\Delta t)_y = -(G^{*}_{j,k+1} - G^{*}_{j,k})/(\Delta y) \tag{17a}$$

where

$$G^{*}_{j,k} = -(T^{*}_{j,k} - T^{*}_{j,k-1})/(\Delta y) \tag{17b}$$

and

$$\left(\overline{\frac{\partial T}{\partial t}}\right)^{**}_{j,k} = -(\bar{G}^{**}_{j,k} - \bar{G}^{**}_{j,k-1})/(\Delta y) \tag{17c}$$

with

$$\bar{G}^{**}_{j,k} = -(\bar{T}^{**}_{j,k+1} - \bar{T}^{**}_{j,k})/(\Delta y) \tag{17d}$$

Then,

$$(T^{**}_{j,k} - T^{*}_{j,k})/(\Delta t)_y = \frac{1}{2}\left[\left(\frac{\partial T}{\partial t}\right)^{*}_{j,k} + \left(\overline{\frac{\partial T}{\partial t}}\right)^{**}_{j,k}\right] \equiv \left[\left(\frac{\partial \bar{T}}{\partial y}\right)^{*}_{j,k}\right]_y \tag{17e}$$

The allowable time step $(\Delta t)_x$ for L_x is determined by the stability requirements for the predictor-corrector steps in (14) or (15) and the allowable time step $(\Delta t)_y$ for L_y is determined by the stability requirements for L_y applying the predictor-corrector steps in (16) or (17).

Symmetry in the sequence for application of the operators was found [7] to produce second order accuracy. For the case that $(\Delta t)_x$ is much larger than $(\Delta t)_y$, the early recommendation [7] was:

$$T_{j,k}^{n+1} = T(x_j, y_k, t + \Delta t) = \left[L_y\left(\frac{\Delta t}{2M}\right)\right]^M [L_x(\Delta t)]\left[L_y\left(\frac{\Delta t}{2M}\right)\right]^M T(x_j, y_k, t) \quad (18)$$

where M is an integer and the exponent indicates the number of applications of L_y before the next operation. For the case that $(\Delta t)_y \gg (\Delta t)_x$, the roles of L_x and L_y in (18) should be interchanged. In a later investigation [8] the following operator sequence was recommended:

$$T_{j,k}^{n+1} = T(x_j, y_k, t + \Delta t) = \left[L_y\left(\frac{\Delta t}{2M}\right) L_x\left(\frac{\Delta t}{M}\right) L_y\left(\frac{\Delta t}{2M}\right)\right]^M T(x_j, y_k, t) \quad (19)$$

The value of 1 for M seems most appropriate if Δt is made sufficiently small.

Two questions became important in the application of these sequences:

1. Can L_y be applied $2M$ times (as in (18)) each time L_x is applied if M is a large number? The same question applies to the appropriate version of (18) for $(\Delta t)_y \gg (\Delta t)_x$.

2. Is there a lower limit upon $(\Delta t)_x$ or $(\Delta t)_y$ which makes (18) or (19) inappropriate?

C. *Stability Analysis of L_y*

As in [2], [7] and [8], a von Neumann stability analysis is applied and the amplification of all Fourier components of a disturbance is examined. Each Fourier component is assumed to have the form:

$$T_{j,k}^n = W^n(t)\,\mathrm{EXP}[i(k_1 x_j + k_2 y_k)] = W^n(t)\,\mathrm{EXP}[i(k_1 j\,\Delta x + k_2 k\,\Delta y)] \quad (20)$$

where $W^n(t)$ is the amplitude at time t and k_1 and k_2 are the wave numbers.

Substitution of (20) into (16) yields:

$$G_{j,k}^* = -(e^{ik_2\Delta y} - 1)\,T_{j,k}^*/(\Delta y)$$

$$\bar{T}_{j,k}^{**} = [1 + 2\xi_y(\cos k_2\,\Delta y - 1)]\,T_{j,k}^*$$

$$\bar{G}_{j,k}^{**} = -\frac{1}{(\Delta y)}(1 - e^{-ik_2\Delta y})[1 + 2\xi_y(\cos k_2\,\Delta y - 1)\,T_{j,k}^* \quad (21a)$$

$$\xi_y = \frac{(\Delta t)_y}{(\Delta y)^2} \quad (21b)$$

Then, the amplification factor for L_y as given by (16) is:

$$G_y = \frac{T^{**}_{j,k}}{T^{*}_{j,k}} = 1 - 2w_y + 2w_y^2, \qquad w_y = \xi_y(1 - \cos k_2 y) \tag{22}$$

The relations for $G^{*}_{j,k}$, $\bar{T}^{**}_{j,k}$ and $\bar{G}^{**}_{j,k}$ differ if (17) is used instead of (16), but (22) is again obtained.

From (22), $| G_y |$ is less than 1 only for w_y from 0 to 1 and equals 1 only at w_y of 0 and 1. Since w_y varies from 0 for $k_2 \Delta y$ equal to 0 or an even multiple of π to $2\xi_y$ for $k_2 \Delta y$ equal to an odd multiple of π, it is apparent that

$$\xi_y = \frac{(\Delta t)_y}{(\Delta y)^2} \leqslant \frac{1}{2} \tag{23}$$

is necessary to satisfy the stability requirement that $| G_y | \leqslant 1$.

D. *Stability Analysis of L_x*

Substitution of (20) into (14) yields

$$F^{*}_{j,k} = [\beta - (e^{ik_1 \Delta x} - 1)]\, T^{*}_{j,k}$$

$$\bar{T}^{**}_{j,k} = [1 - \eta\xi_x\beta(1 - e^{-ik_1\Delta x}) + \xi_x(e^{ik_1\Delta x} - 2 + e^{-ik_1\Delta x})]\, T^{*}_{j,k}$$

$$\bar{F}^{**}_{j,k} = [\beta - (1 - e^{-ik_1\Delta x})\,\Delta x][1 - \xi_x\eta(1 - e^{-ik_1\Delta x}) + \xi_x(e^{ik_1\Delta x} - 2 + e^{-ik_1\Delta x})]\, T^{*}_{j,k}$$

with the amplification factor given by

$$G_x \equiv \frac{T^{**}_{j,k}}{T^{*}_{j,k}} = [1 + \xi_x(2 + \eta^2\xi_x)(\cos k_1 \Delta x - 1) + 2\xi_x^2(\cos k_1 \Delta x - 1)^2] - in\xi_x \sin k_1 \Delta x\, [1 + 2\xi_x(\cos k_1 \Delta x - 1)]$$

$$\equiv \mathrm{Re}(G_x) + i\,\mathrm{Im}(G_x) \tag{24}$$

where

$$\eta = \beta \Delta x, \qquad \xi_x = \frac{(\Delta t)_x}{(\Delta x)^2} \tag{25}$$

Then,

$$| G_x |^2 = [\mathrm{Re}(G_x)]^2 + [\mathrm{Im}(G_x)]^2 = \sum_{i=0}^{4} A_i(\cos k_1 \Delta x)^i \tag{26}$$

where

$$A_0 = 1 - 4\xi_x + (8 - \eta^2)\,\xi_x^2 - 8\xi_x^3 + (\eta^4 + 4)\,\xi_x^4 \tag{27a}$$

$$A_1 = 4\xi_x + 2(\eta^2 - 8)\,\xi_x^2 + 4(6 - \eta^2)\,\xi_x^3 - 2(\eta^4 - 2\eta^2 + 8)\,\xi_x^4 \tag{27b}$$

$$A_2 = (8 - \eta^2)\,\xi_x^2 + 8(\eta^2 - 3)\,\xi_x^3 + (\eta^4 - 12\eta^2 + 24)\,\xi_x^4 \tag{27c}$$

$$A_3 = 4(2 - \eta^2)\,\xi_x^3 + 4(3\eta^2 - 4)\,\xi_x^4 \tag{27d}$$

$$A_4 = 4(1 - \eta^2)\,\xi_x^4 \tag{27e}$$

From (20) and (15), different formulas for $F_{j,k}^{*}$, $\bar{T}_{j,k}^{**}$ and $\bar{F}_{j,k}^{**}$ result. However G_x is again given by (24). The final step is to choose $(\Delta t)_x$ such that

$$| G_x |^2 \leqslant 1 \tag{28}$$

for all possible values of the other parameters (β, Δx, and k_1).

From (26), $| G_x |^2$ is a periodic function of $k_1 \Delta x$ and hence $| G_x |^2$ has maxima and minima which are clearly functions of η and ξ_x. Therefore, one possible approach to ensure stability is to choose ξ_x (hence $(\Delta t)_x$ for a given problem) such that the maxima are all less than 1. The first step must be to find the Fourier components (values of k_1) for the extrema of $| G_x |^2$. Next, the Fourier components producing maxima must be separated from the Fourier components for all extrema. Finally, ξ_x must be determined as a function of η such that the largest magnitude for all maxima is less than one.

The smallest wave length, $(l_1)_{\min}$, which can be supported by the grid places the node points of the wave at the grid points such that

$$(l_1)_{\min} = 2\Delta x \tag{29}$$

As a result the maximum wave number possible is

$$(k_1)_{\max} = \frac{2\pi}{(l_1)_{\min}} = \frac{\pi}{\Delta x} \qquad \text{or} \qquad (k_1)_{\max}\,\Delta x = \pi \tag{30}$$

Extrema, which may be maxima or minima occur for the values of k_1 producing

$$\begin{aligned} 0 = \frac{\partial}{\partial k_1} | G_x |^2 &= 2[\mathrm{Re}(G_x)]\,\frac{\partial}{\partial k_1}[\mathrm{Re}(G_x)] + 2[\mathrm{Im}(G_x)]\,\frac{\partial}{\partial k_1}[\mathrm{Im}(G_x)] \\ &= -\left[\sum_{i=1}^{4} iA_i(\cos k_1 \Delta x)^{i-1}\right](\sin k_1 \Delta x)\,\Delta x \end{aligned} \tag{31}$$

An extremum will be a maximum if

$$\begin{aligned} \frac{\partial^2}{\partial k_1^2} | G_x |^2 &= (\Delta x)^2 \{2A_2 + (6A_3 - A_1)(\cos k_1 \Delta x) \\ &\quad + 4(3A_4 - A_2)(\cos k_1 \Delta x)^2 - 9A_3(\cos k_1 \Delta x)^3 - 16A_4(\cos k_1 \Delta x)^4\} \\ &= 2[\mathrm{Re}(G_x)]\,\frac{\partial^2}{\partial k_1^2}[\mathrm{Re}(G_x)] + 2\left\{\frac{\partial}{\partial k_1}[\mathrm{Re}(G_x)]\right\}^2 \\ &\quad + 2[\mathrm{Im}(G_x)]\,\frac{\partial^2}{\partial k_2^2}[\mathrm{Im}(G_x)] + 2\left\{\frac{\partial}{\partial k_1}[\mathrm{Im}(G_x)]\right\}^2 \leqslant 0 \end{aligned} \tag{32}$$

It is apparent from (31) that the Fourier components with $sink_1 \Delta x = 0$ will produce extrema. In view of the restriction in (30), the wave numbers of interest for extrema are

$$k_1 \Delta x = m\pi \qquad \text{where} \quad m = 0 \text{ or } 1 \tag{33}$$

From (24) and (33), G_x at these extrema locations is real and given by

$$G_{x_{\text{EXT}}} = 1 + (2\xi_x + \eta^2\xi_x^2)[(-1)^m - 1] + 2\xi_x^2[(-1)^m - 1]^2 \tag{34}$$

Then, using (32) and (34), an extremum may be a maximum if

$$\frac{1}{(\Delta x)^2}\left(\frac{\partial^2}{\partial k_1^2} \mid G_x \mid^2\right)_{\text{EXT}} = 2G_{x_{\text{EXT}}}(-1)^{m+1}\{2\xi_x + \eta^2\xi_x^2 + 4\xi_x^2[(-1)^m - 1]\} + 2\eta^2\xi_x^2\{1 + 2\xi_x[(-1)^m - 1]\}^2 \leqslant 0 \tag{35}$$

When m is zero,

$$G_{x_{\text{EXT}}} = 1 \tag{36}$$

$$\left(\frac{\partial}{\partial k_1^2} \mid G_x \mid^2\right)_{\text{EXT}} = -4(\Delta t)_x = -4\xi_x(\Delta x)^2 \tag{37}$$

Since the latter is always negative, this extremum is a maximum and the Fourier component with m equal to zero has the marginal stability requirement ($\mid G_{x_{\text{EXT}}} \mid = 1$) for all $(\Delta t)_x$.

For m equal to 1,

$$G_{x_{\text{EXT}}} = 1 - 2(2\xi_x + \eta^2\xi_x^2) + 8\xi_x^2 \tag{38}$$

$$\frac{1}{(\Delta x)^2}\left(\frac{\partial^2}{\partial k_1^2} \mid G_x \mid^2\right)_{\text{EXT}} = 2G_{\text{EXT}}[2 + \eta^2\xi_x^2 - 8\xi_x^2] + 2\eta^2\xi_x^2(1 - 4\xi_x)^2 \tag{39}$$

The solid curves on Figure 1 indicate the boundaries where $\mid G_x \mid^2_{\text{EXT}} = 1$ and $\{(\partial^2/\partial k_1^2) \mid G_x \mid^2\} = 0$. The arrows extending from these curves designate the regions where the extremum may be acceptable, i.e. $\mid G_x \mid^2 < 1$, and where the extremum is a maximum. It is apparent that this extremum is not a maximum for a region $1.1 \leqslant \eta \leqslant 2.2$. Furthermore in this region, the locations (ξ_x) of the extremum may be double and triple valued with a very thin region between the curves with $\mid G_x \mid^2 \leqslant 1$ but a maximum is not predicted.

Further understanding is enhanced by considering two limiting cases:

a. no convection ($\beta = 0$)

b. no thermal diffusion.

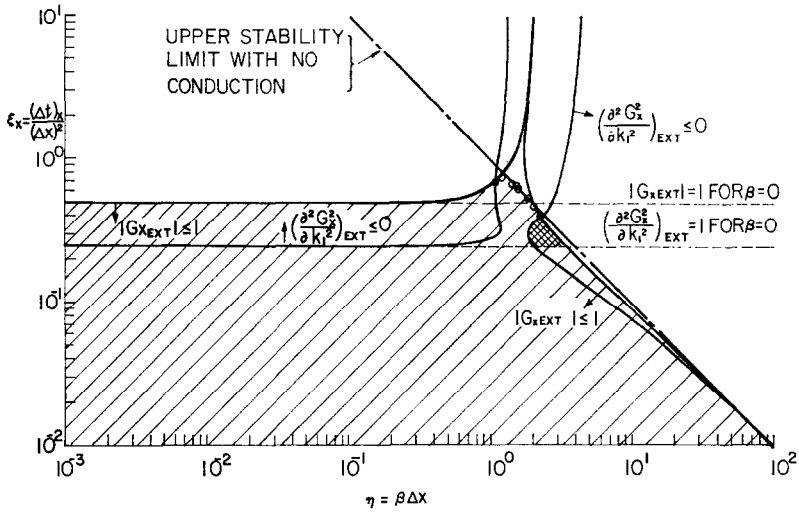

FIG. 1. Stability limits for the L_x operator.

The first limiting case is actually the stability problem for G_y and the results from the previous analysis are the dotted lines on Figure 1. This result is of course not a function of β but is spread over the entire range of β of Figure 1 merely to show that this limit is very practical for $\beta\,\Delta x$ less than 0.2.

The limiting case with no thermal diffusion is obtained from (24) merely by neglecting all terms involving ξ_x but not η. Then,

$$|\,G_x\,|^2 = 1 + (\alpha^2 - \alpha)\,\omega_x \tag{40}$$

$$w_x = 1 - \cos k_1\,\Delta x, \qquad \alpha = \eta^2 \xi_x^2 \tag{41}$$

Since w_x is always positive, $|\,G_x\,|^2 \leqslant 1$ only if $\alpha^2 - \alpha = \alpha(\alpha - 1)$ is negative. By definition, α is always positive. Therefore, stability requires $\alpha < 1$ or

$$\frac{(\Delta t)_x}{(\Delta x)^2} = \xi_x < \frac{1}{\eta} = \frac{1}{\beta\,\Delta x} \tag{42}$$

The upper stability limit for this case is shown on Figure 1 to be a natural asymptote of the more general case for large β.

Only the roots of (31) producing $\sin k_1\,\Delta x = 0$ have been examined to this point. The roots corresponding to the remaining possibilities (contents of the square bracket in (31)) were investigated next. These roots are obtained from the cubic equation

$$A_1 + 2A_2 \cos k_1\,\Delta x + 3A_3 \cos^2 k_1\,\Delta x + 4A_4 \cos^3 k_1\,\Delta x = 0 \tag{43}$$

It is apparent that these roots will be functions of η and ξ_x and that (32) must be applied to separate the maxima. Analytical solutions of (43) could not be found and a

computer program was used to scan the range of ξ_x and η on Figure 1 for maxima.

With η fixed at a value less than 0.4, the roots of (43) have $\cos k_1 \Delta x > 1$ with no real k_1 for $\xi_x < 0.25$. Then a minimum occurs near $k_1 \Delta x = \pi$ for ξ_x slightly larger than 0.25 and moves toward $k_1 \Delta x = 0$ as ξ_x increases. With the results of Figure 1, it is apparent that for $\xi_x \leqslant 0.25$, $| G_x |$ will decrease from a maximum of 1 at $k_1 \Delta x$ of 0 to a minimum at $k_1 \Delta x = \pi$. For $0.25 < \xi_x$, $| G_x |$ will decrease from 1 at $k_1 \Delta x$ of 0 to a minimum. Then $| G_x |$ will increase to a maximum, which is greater than or equal to 1 for $\xi_x \geqslant 0.5$, at $k_1 \Delta x$ of π.

Therefore, with ξ_x below the curve for $| G_{x_{\text{EXT}}} | = 1$ and η less than 0.4, stable calculations should result. For $0.4 < \eta < 1.1$, the variation of $| G_x |$ with ξ_x at fixed η is qualitatively the same as for smaller η expect that the minimum for $0 < k_1 \Delta x < \pi$ does not occur until ξ_x is above the curve for $((d^2/dk_1^2)| G_x |)_{\text{EXT}} = 0$. Stability still occurs for ξ_x below the curve for $| G_{x_{\text{EXT}}} | = 1$.

For a fixed η in the range $1.1 < \eta < 2.2$, $| G_x |$ decreased from a maximum of 1 at $k_1 \Delta x = 0$ to an minimum at $k_1 \Delta x = \pi$ where ξ_x is a small number. For ξ_x fixed above some threshold value and for increasing $k_1 \Delta x$, $| G_x |$ decreases from a maximum of 1 at $k_1 \Delta x = 0$ to a minimum, increases to a maximum, and decreases to a minimum at $k_1 \Delta x = \pi$. The values of ξ_x where the maximum is 1 are indicated by the circles on Figure 1.

When η is fixed at a value greater than 2.3, the variation of $| G_x |$ with $k_1 \Delta x$ is qualitatively the same as when $\eta < 1.1$. $k_1 \Delta x = 0$ is always the location of the maximum with $| G_x | = 1$ and $k_1 \Delta x = \pi$ is the location of a minimum for ξ_x below the curve for $(d^2 G_x^2/dk_1^2)_{\text{EXT}} = 0$. For larger ξ_x, a minimum occurs for $0 < k_1 \Delta x < \pi$ and a maximum occurs at $k_1 \Delta x = \pi$. With ξ_x below the curve for $| G_{x_{\text{EXT}}} | = 1$, the maximum at $k_1 \Delta x = \pi$ is less than 1 but, when ξ_x is larger, the maximum is greater than 1.

In summary, the above analysis shows that the stable region for L_x is the shaded region on Figure 1 given by the following criteria:

(a) For $\beta \Delta x = \eta \leqslant \eta_l$,

$$(\Delta t)_x/(\Delta x)^2 < \{\xi_x \text{ for } | G_x |^2_{\text{EXT}} = 1 \text{ with } k_1 \Delta x = \pi\} \tag{44a}$$

(b) For $\eta_l \leqslant \beta \Delta x \leqslant \eta_u$,

$$(\Delta t)_x/(\Delta x)^2 < \frac{1}{\beta \Delta x} \tag{44b}$$

(c) For $\eta_u \leqslant \beta \Delta x$,

$$(\Delta t)_x/(\Delta x)^2 < \{\xi_x \text{ for } | G_x |^2_{\text{EXT}} = 1 \text{ with } k_1 \Delta x = \pi\} \tag{44c}$$

where η_l and η_u are the lower and upper values of η at the intersections of the curves on Fig. 1 where $| G_x |^2_{\text{EXT}} = 1$ for $k_1 \Delta x = \pi$ with and without conduction. However, it is also apparent from Figure 1 that a more practical and much less complicated upper stability boundary is formed by using the smaller of the values of $\xi_x = (\Delta t)_x/$

$(\Delta x)^2$ where $| G_x |^2_{\text{EXT}} = 1$ at fixed $\eta = \beta \Delta x$ for the limiting cases of no conduction or no convection, i.e.,

$$\frac{(\Delta t)_x}{(\Delta x)^2} = \text{the smaller of } 0.5 \text{ or } \frac{1}{\beta \Delta x} \tag{45}$$

E. *Impact of Stability Requirements Upon the Time-Split Algorithm*

The stability analysis here requires that L_x and L_y have upper but not lower stability bounds. Therefore, the operations in (18) and (19) are not limited by the second question in Section IIB. The first question in Section 11B is best resolved by numerical experiments.

III. Numerical Experiments

All numerical experiments were conducted for the problem in (1) to (5) with:

$$T_\infty = 1, g(y) = 1.5 - 0.5 \cos(\pi y) \tag{46}$$

Then, the exact solution is obtained from (8) with

$$T_\infty = 1, (\delta T)_1 = 0.5, (\delta T)_2 = -0.5$$

The conduction problem of [1] was modified to apply the L_x operator of (14) and the L_y operator of (16) in the following operator sequence:

$$T^{n+1}_{j,k} = [L_y(\Delta t)_y]^M [L_x(\Delta t)_x][L_y(\Delta t)_y]^M T^n_{j,k} \tag{47}$$

$$\Delta t = (\Delta t)_x = 2M(\Delta t)_y, t^{n+1} = t^n + \Delta t \tag{48}$$

Then, by individually varying M, $(\Delta t)_x$ and $(\Delta t)_y$ the algorithms in (18) and (19) can be tested and the validity of the stability boundaries can be verified.

A figure of merit for the comparison of exact and numerical solutions is the relative error given by:

$$E^n_{j,k} = |[T^n_{j,k} - T_{\text{EXACT}}(x_j, y_k, t^n)]/[g(1) - g(0)]| \tag{49}$$

This relative error was calculated at every computational point in space and after each time cycle as the nomenclature indicates. Since the amount of data to be scanned for this comparison would be quite large with this figure of merit, the figure of merit used in the graphs is

$$E_{\text{MAX}}(t^n) = \text{the maximum value of } E^n_{j,k} \text{ at } t^n \tag{50}$$

Because the stability of L_x is much more complicated, the value of $(\Delta t)_x$ was first varied parametrically using a "safe" value of $(\Delta t)_y$. Ten intervals ($K11 = 10$) is a practical choice for the y range (0 to 1). Therefore, in accordance with (23) the stable

TABLE 1

Summary of Checkout Runs

Case	$\beta\Delta x$	$(\Delta t)_x$	$(\Delta t)_y$	M	T_s	$\xi_x = \frac{(\Delta t)_x}{(\Delta x)^2}$	$\xi_y = \frac{(\Delta t)_y}{(\Delta y)^2}$	Comment
1	2.45	0.056	0.004	7	0.911	0.4571	0.4	Above stab. boundary/unstable
2	2.45	0.048	0.004	6	0.911	0.3918	0.4	just below the upper stabl. bdry.
3	2.45	0.040	0.004	5	0.911	0.3265	0.4	center of darkly shaded region
4	2.45	0.032	0.004	4	0.911	0.2612	0.4	in darkly shaded region
5	2.45	0.024	0.004	3	0.911	0.1959	0.4	below darkly shaded region
6	2.45	0.008	0.004	1	0.911	0.06531	0.4	special case of (19)
7	2.45	0.04	.0066667	3	0.911	.3265	.6667	above the upper stab. bdry.
8	2.45	0.04	.005	4	0.911	.3265	.5	at the upper stability bdry.
9	2.45	0.04	.002	10	0.911	.3265	.2	well below the upper stab. bdry.
10	0.35	.072	.004	9	9.0	.5878	.4	above the stability boundary
11	0.35	.064	.004	8	9.0	.5225	.4	at the stability boundary
12	0.35	.024	.004	3	9.0	.1959	.4	well below the stability boundary
13	1.6	0.20	.004	25	1.632	1.6327	.4	well above the stability boundary
14	1.6	0.088	.004	11	1.632	.7184	.4	above the stability boundary
15	1.6	0.08	.004	10	1.632	.6531	.4	slightly above the stab. bdry.
16	1.6	0.008	.004	1	1.632	.06531	.4	well below the stab. bdry.
17	1.95	1.12	0.004	140	1.232	9.1429	.4	ξ_x is in the upper region
18	1.95	.12	0.004	15	1.232	.9796	.4	well above upper stability bdry.
19	1.95	0.064	0.004	8	1.232	.5224	.4	above upper stability boundary.
20	1.95	0.056	0.004	7	1.232	.4571	.4	below upper stability boundary.
21	1.95	0.008	0.004	1	1.232	.06531	.4	well below upper stability bdry.
22	8.75	0.016	0.004	2	0.208	.1306	.4	above upper stability boundary.
23	8.75	0.008	0.004	1	0.208	.06531	.4	well below upper stab. bdry.

range for L_y is $(\Delta t)_y < 0.5(.1)^2 = .005$ and a "safe", convenient value in the stable range is

$$(\Delta t)_y = 0.004 \tag{51}$$

Note, that the appropriate stability region for the corresponding case (odd harmonics) in the unpublished stability analysis of the MacCormack algorithms used in [1] is the darkly shaded region in the range $1.8 < \beta\,\Delta x < 3.4$. Since comparison with those results was desired, $\Delta x = 0.35$ was chosen to produce a point close to the center of that region with $\beta = 7$. Ten intervals in the x direction then produces a maximum x of 3.5. With $(\Delta t)_y$ fixed, variation of M implies variation of $(\Delta t)_x$ consistent with (48) which produces the required symmetry of (47).

As shown on Table I, a series of checkout runs were made at $\beta\,\Delta x = 2.45$ with $(\Delta t)_y$ fixed at 0.004 and M varying from 7 to 1. Then, $(\Delta t)_x/(\Delta x)^2$ varies from values above the upper stability boundary (0.41) to values significantly below the lower bound of the darkly shaded region. For $M = 7$, which has $(\Delta t)_x$ just above the upper boundary, instability occurred quickly as predicted. As shown in Figure 2, the algorithm was unstable for $M = 6$ with $(\Delta t)_x$ just below the upper stability boundary. For smaller M, stable solutions were obtained. The case with $M = 3$ has $(\Delta t)_x$ just below the lower limit of the darkly shaded region and, for $M = 1$, $(\Delta t)_x$ is much below this lower limit. As M decreases below 5 no improvement in stability is obtained but accuracy does improve. Also shown in Table 1 is the parameter T_s which is the time required to obtain a reasonable approach to steady state at the downstream location $x = x_{\max}$, i.e. when

$$(T - \text{steady state } T)/(\text{initial } T - \text{steady state } T) \leqslant 0.01$$

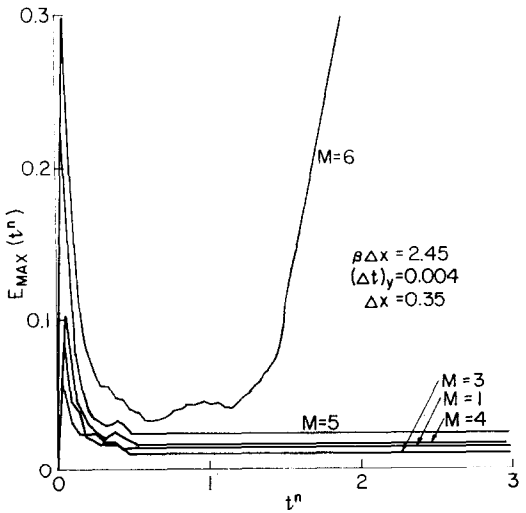

FIG. 2. Maximum relative error for Cases 1 through 6.

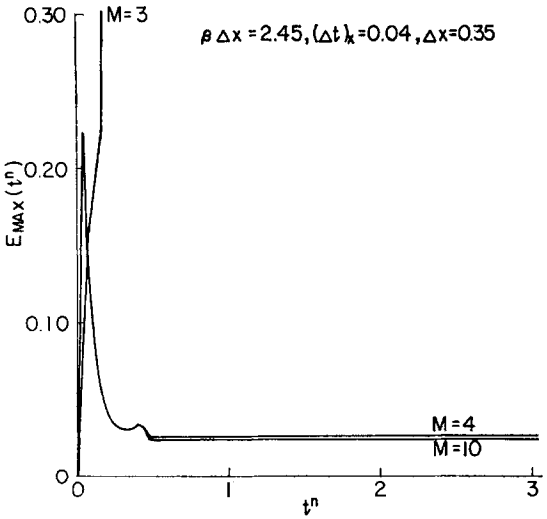

FIG. 3. Maximum relative error for Cases 7 through 9.

Cases 7 to 9, as shown on Figure 3, test the validity of (23) with $(\Delta t)_x$ fixed at the largest value producing stability in the previous sequence. For $M = 3$, the value of $(\Delta t)_y$ is above the predicted upper stability limit and the results clearly demonstrate instability. For the next smaller $(\Delta t)_y$ with $M = 4$, a stable solution was obtained. A much smaller $(\Delta t)_y$ with $M = 10$ produces little improvement in stability or accuracy.

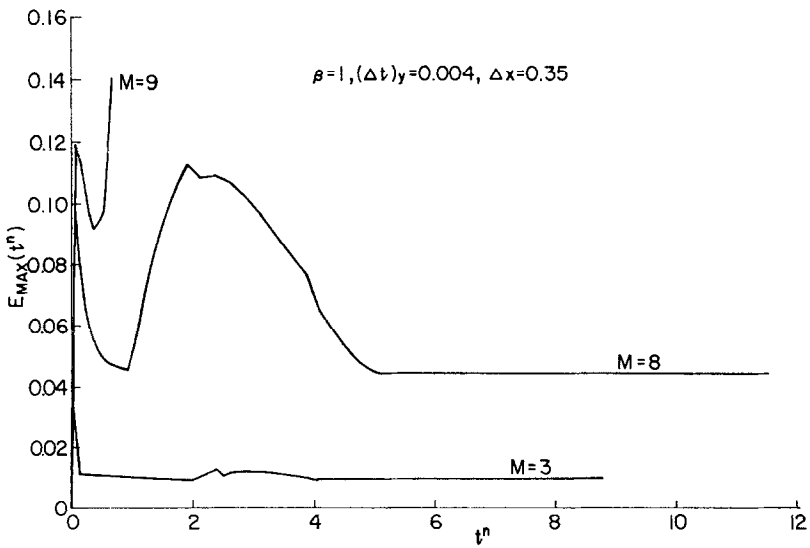

FIG. 4. Maximum relative error for Cases 10 through 12.

The upper stability boundary for L_x was then checked for a value of β in each range of importance as shown on Figure 1. For $\beta\,\Delta x \leqslant 0.2$, the upper stability boundary is constant ($\xi_x = 0.5$). With $\beta = 1$, the upper stability boundary has $\xi_x \approx 0.52$ from Figure 1. Cases 10 to 12 of Table I and Figure 4 verify this prediction. Case 10 for $M = 9$ has ξ_x above this value and instability occurs. When $M = 8$ (Case 11), ξ_x is at this boundary and the solution is marginally stable. A stable solution is obtained for Case 12 when ξ_x is well below this limit.

For $\beta\,\Delta x = 1.6$ (Cases 13 to 16), the upper stability limit from Fig. 1 is $\xi_x = .64$. The results shown on Figure 5 and in Table 1 show that instability occurs for ξ_x significantly above this value ($M = 11$ and 25). However, for $M = 10$ where ξ_x is slightly above this limit, stability appears to be achieved. For $M = 1$, which has ξ_x significantly below the limit, the solution is stable and accurate.

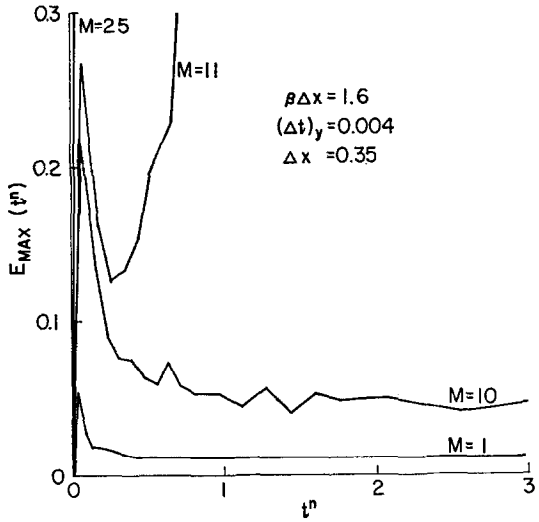

FIG. 5. Maximum relative error for Cases 13 through 16.

Cases 17 to 21 of Table 1 and Figure 6 test the stability boundary at $\beta\,\Delta x = 1.95$ which is in the range where the stability boundary is determined by the roots of (43). At this $\beta\,\Delta x$, $M = 140$ produces a value of ξ_x which is in the upper region with $| G_{x_{\text{EXT}}} | < 1$ but the extremum is a minimum. $M = 15$ and 8 produces values of ξ_x which are in the upper right region with $| G_{x_{\text{EXT}}} | > 1$. Instability occurred almost immediately for cases 17 and 18 and is developing for $M = 8$. For $M = 1$ and 7, ξ_x is well below the upper stability limit of 0.52 and stable solutions were obtained.

The last two cases of Table 1 and Figure 7 have $\beta\,\Delta x$ well into the region where the influence of conduction is negligible. The upper limit (0.11) is exceeded for $M = 2$ and instability occurs. When $M = 1$, ξ_x is well below the stability limit and stable solutions are obtained.

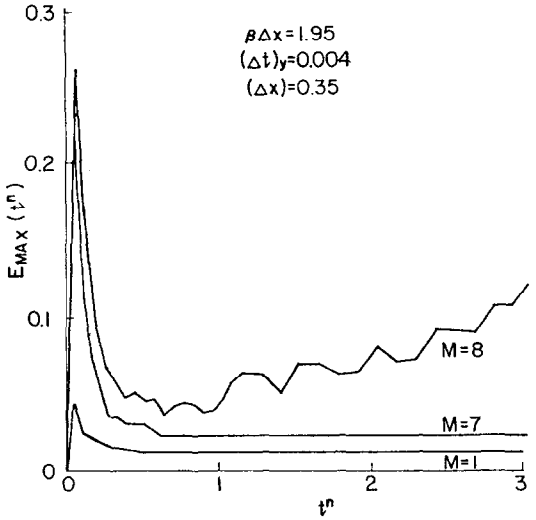

FIG. 6. Maximum relative error for Cases 17 through 21.

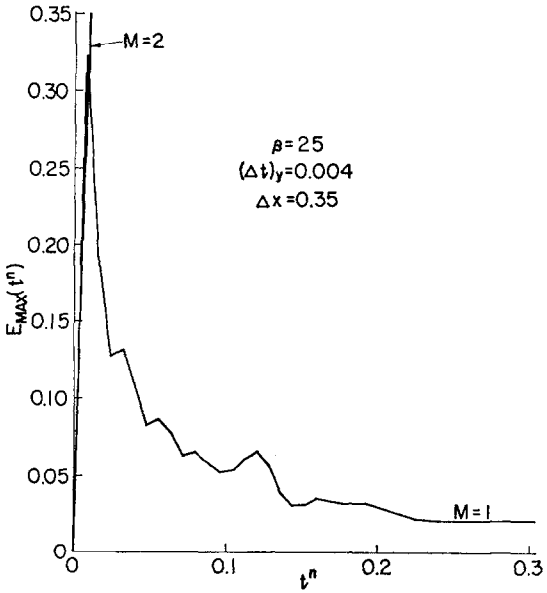

FIG. 7. Maximum relative error for Cases 22 and 23.

IV. Discussion of the Results and Conclusions

Question 1 of Section IIB has been answered in that stable solutions were obtained in the numerical experiments with the time split method for large values of M if the upper stability limit is not exceeded. Unlike the results for an unpublished stability

analysis of the original MacCormack method [2], no lower stability limit was predicted by the present stability analysis. Furthermore, the numerical experiments for the time split method verified this finding. Therefore, question 2 in Section IIB has also been resolved and no complicating lower limit exists.

The examination of extrema in the amplification factor was very useful in defining the stability boundary over the entire range of parameters of interest. However, this technique was most useful for the range of parameters where the maxima did not occur for Fourier components with wave numbers of 0 or 1. For the conduction problem examined here, this range was not extensive and the approximate stability boundary of (45), which is an obvious choice in the absence of this analysis, appears to be reasonable. However, accurate determination of the stability boundaries may be much more crucial in other problems and examination of extrema in the amplification would have more importance.

ACKNOWLEDGMENTS

This research was initiated and partially completed with the sponsorship of the Minta Martin Fund for Aeronautical Research, an endowment given to the College of Engineering by the late Glenn L. Martin. The research was completed with the support of ONR Contract N00014-77-C-0257 monitored by Mr. Morton Cooper. Support of the Computer Science Center at the University of Maryland was also essential. The comments and suggestions of the reviewers were very helpful and are appreciated. The patience of Sue Osborn in typing the manuscript and revisions was essential.

REFERENCES

1. E. JONES AND J. D. ANDERSON, JR., "Numerical Solution of the Navier–Stokes Equations for Laminar and Turbulent Supersonic Mixing Flows," Department of Aerospace Engineering Technical Report No. AE 75-5, University of Maryland, 1975.
2. R. W. MACCORMACK, "The Effects of Viscosity in Hypervelocity Impact Cratering," AIAA Paper No. 69-354, 1969.
3. R. BORGHI AND M. CHARPENEL, *Astronaut Acta.* **17** (1972), 833–842, (in French).
4. M. D. GRIFFIN, J. D. ANDERSON, JR., AND R. DIWAKAR, *AIAA J.* **14** (1976), 1665.
5. R. DIWAKAR, J. D. ANDERSON, JR., M. D. GRIFFIN, AND E. JONES, *AIAA J.* **14** (1976), 1667.
6. R. D. RICHTMYER AND K. W. MORTON, "Difference Methods for Initial-Value Problems," Interscience, 1967.
7. R. W. MACCORMACK, *Lecture Notes in Physics*, Vol. 8, 151–163, Springer-Verlag, 1971.
8. B. S. BALDWIN, R. W. MACCORMACK, AND G. S. DEIWERT, "Notes for Short Course in Computational Methods for Inviscid and Viscous Two and Three Dimensional Flows," 2-1, to 2-24, Fluid Dynamics Institute, Hanover, N.H., 1975.